ELSEVIER

Thin Solid Films 368 (2000) 74–79

thin solid films

www.elsevier.com/locate/tsf

Characterization of amorphous aluminum oxide films prepared by the pyrosol process

A. Ortiz[a,*], J.C. Alonso[a], V. Pankov[a], A. Huanosta[a], E. Andrade[b]

[a]*Instituto de Investigaciones en Materiales, UNAM, A.P. 70-360, Coyoacán 04510, D.F., Mexico*
[b]*Instituto de Física, UNAM, A.P. 20-364, Coyoacán 01000, D.F., Mexico*

Accepted 26 January 2000

Abstract

Amorphous aluminum oxide films were deposited by the pyrosol process using aluminum acetylacetonate as source material dissolved in a mixture of three parts of deionized water and one part of methanol. An accelerator ion beam analysis technique was used to obtain the areal density and the chemical composition of the aluminum oxide films, which result in being oxygen-rich when films are deposited at a substrate temperature of 480°C. The infrared spectra show a broad-absorption band from 400 to 1000 cm^{-1} typical of the vibrations of the Al_2O_3. IR analysis also shown that there are no O–H or alanol (Al–OH) groups incorporated in the films and that films kept at air atmosphere at room temperature have a high stability against water adsorption. The refractive index of the films measured by ellipsometry was 1.647. The optical transmission has a value of the order of 88% in the range from 400 to 900 nm for films deposited onto pyrex glass and fused quartz slices. There is no optical absorption edge for wavelengths around 190 nm, which indicates that the deposited films have an energy band gap of at least 6.2 eV. The current density-electric field characteristics of MIM structures, incorporating insulating aluminum oxide films, show current injection across the film for electric fields higher than 2 MV/cm. Electric breakdown was not observed for applied electric fields of the order of 4.5 MV/cm.

Keywords: Aluminum oxide; Dielectrics; Insulators; Pyrolysis

1. Introduction

Aluminum oxide has excellent and stable chemical and physical characteristics. This material has a high thermal conductivity, high resistance to radiation and high resistance to corrosion, thus aluminum oxide films have been applied as a protective coating [1]. Due to its electrical characteristics, thin films of this material have been applied as insulator layer in electronic devices, such as MOS field effect transistors and electroluminescent panels [2]. The application in electroluminescent (EL) structures is important due to its high dielectric constant and low permeability to alkali ions. It is known that the purpose of insulator layers in EL devices, of the MISIM type, are to protect the phosphor layer from electric breakdown, to prevent the metal-ion diffusion into the active layer and to provide interface states at the boundary between the phosphor layer and the insulator layer. To accomplish these purposes the insulator layers must have the following characteristics: (i) high breakdown electric field, (ii) high dielectric constant, (iii) good adhesiveness, (iv) a small number of pinholes and (v) small $\tan\delta$ [3]. In general, aluminum oxide films, prepared by several methods using different source materials, have microstructural and electrical characteristics suitable to be applied in electroluminescent devices. On the other hand, porous anodic aluminum oxide thick films have been applied in the preparation of humidity sensors [4].

Some of the methods to deposit Al_2O_3 films using different source materials, are: (1) chemical vapor deposition using aluminum acetylacetonate in an air atmosphere with a deposition rate of 15 A/min – in order to increase the deposition rate it was observed that water vapor must be used as source material [5]; (2) low-pressure MOCVD using a mixture of Tris(2,2,6,6-tetramethylheptane-3,5-dionate) aluminum complex, O_2, Ar and Ar/H_2O [6]; (3) electron beam evaporation of alumina [7]; (4) phosphorus-doped aluminum oxide films deposited by atomic layer epitaxy using aluminum *n*-propoxide and deionized water [8]; (5) the preparation of photoluminescent aluminum oxide films by the pyrosol process using aluminum acetylacetonate dissolved in a mixture of deionized water and methanol, as reported recently [9]. In that case, the deposited films show photoluminescent emission with a peak

* Corresponding author. Tel.: +52-5-622-4599; fax: +52-5-616-1251.
E-mail address: aortiz@servidor.unam.mx (A. Ortiz).

0040-6090/00/$ - see front matter
PII: S0040-6090(00)00864-6

located at 410 nm for films deposited from 340 to 440°C at air atmosphere. Films deposited at higher substrate temperatures do not show any photoluminescent emission. The pyrosol process has been well described in several reports [10,11] and it has been used to prepare thin films of several materials such as metals, sulfides and oxides. Probably the pyrosol process is the easiest and lowest cost, nonvacuum technique to prepare thin films over large areas.

In this work we report the microstructural and electrical characteristics of aluminum oxide thin films deposited by the pyrosol process using aluminum acetylacetonate dissolved in a mixture of deionized water and methanol at air atmosphere. This method is similar to that reported earlier [9]. The aluminum acetylacetonate is an organometallic compound which is inexpensive, nontoxic and stable in an air atmosphere at room temperature.

2. Experimental

The aluminum oxide films were deposited by the pyrosol process. The start solution was 0.05 M aluminum acetylacetonate (AlAAc) in a mixture of three parts of deionized water and one part of methanol. To obtain the complete dissolution of the AlAAc, 3 ml of acetic acid was added per liter of start solution. The substrate temperatures used were 480 and 510°C. The substrates used in this work were pyrex glass slices, fused quartz slices and glass slices coated with antimony doped tin oxide transparent conducting contact. These substrates were ultrasonically cleaned with trichloroethylene, acetone and methanol. For IR, ellipsometry and Rutherford backscattering measurements (100) *n*-type silicon single crystal slices with 200 Ω cm were used. To remove the native oxide from the c-Si wafers they were chemically etched with P solution (H_2O (300 ml), HNO_3 (10 ml), HF (15 ml)). The deposition time was varied from 5 to 30 min. The carrier gas flow rate was 3.5 l/min and the director gas flow rate was 1.5 l/min, being air for both cases. The films deposited onto pyrex glass were used to measure the thickness, in these cases a small part of the substrate was covered with a cover pyrex glass to form a step during deposition. The thickness of the deposited films was measured with a Sloan Dektac IIA profilometer. The refractive index and thickness of the films were measured by means of a Gaertner 117A ellipsometer using the 632 nm line from a He–Ne laser. The crystallinity of the samples was analyzed by means of a Siemens D500 diffractometer, although all the analyzed samples were of amorphous nature. Ion beam analysis (IBA) methods allow to determine not only the elemental composition of the sample but also the concentration depth profile of the constituent atoms. The IBA facilities at the University of Mexico [12] based on a vertical single-ended 5.5 MeV Van der Graaff accelerator were used to obtain the atomic density (atoms/cm^2) and the composition of the aluminum oxide films. In order to obtain complete information about the films two particle beams were used to bombard the samples: $^4He^+$ and $^2H^+$. A conventional Rutherford backscattering (RBS) technique with a 1.7 MeV $^4He^+$ beam with detector set at $\theta = 170°$ and a nuclear reaction (NR) technique with 0.94 MeV $^2H^+$ beam with detector set at $\theta = 165°$, were used to analyze the films. A surface barrier detector and standard electronics were used to obtain the particle energy spectra. An accurate determination of the oxygen concentration in the films is crucial in this work and a deuterium beam was used to induce the NR: $^{16}O(d,p_0)O^{17}$ and $^{16}O(d,p_1)O^{17}*$. They were used to obtain the oxygen concentration. The RBS and NR oxygen measurements are discussed next. Infrared (IR) transmittance measurements were made with a Fourier transform IR (FTIR) 205 Nicolet spectrophotometer. Optical transmission measurements in the range from 190 to 1100 nm were carried out with a double-beam Shimadzu UV–vis 260 spectrophotometer for the samples deposited onto fused quartz and onto pyrex glass, with air in the reference beam. To evaluate the electrical characteristics of the aluminum oxide films deposited onto the transparent conductive contact, both materials were contacted with aluminum dots deposited by vacuum thermal evaporation; the diameter of the dots was 1.12 mm forming a metal/insulator/metal structure. The electric contacts were made by means of gold-coated tungsten needles supported by micromanipulators to assure ohmic contact. Current–voltage data were obtained with a computer interfaced arrangement incorporating a Kithley 485 picoammeter and a Keithley 230 programmable voltage source.

3. Results and discussion

Fig. 1 shows the variation of the thickness of the deposited films as a function of the deposition time for a substrate temperature of 480°C. From this curve a deposition rate of the order of 17.0 nm/min is obtained. This value is relatively high in comparison with those obtained by means of several deposition techniques [13]. This relatively high value for the deposition rate is explained taking into account the composition of the solvent used, three parts of deionized water and one part of methanol, which has a major component of water. This fact avoids the necessity of addition of a water mist of vapor during the process, and also permits a better oxidation of the aluminum atoms, resulting in films with good structural and electrical properties as will be shown later.

From the ellipsometric measurements the values of the refractive index, $n = 1.647$ and 1.648 for films deposited at substrates temperatures of 480 and 510°C, respectively, are similar to those reported for amorphous films prepared by other techniques [14]. These refractive index values permit to infer that the deposited films, in the present work, have a dense structure as has been shown for aluminum oxide films with refractive index values in the range from 1.61 to 1.73. Table 1 shows the values of the refractive index and the

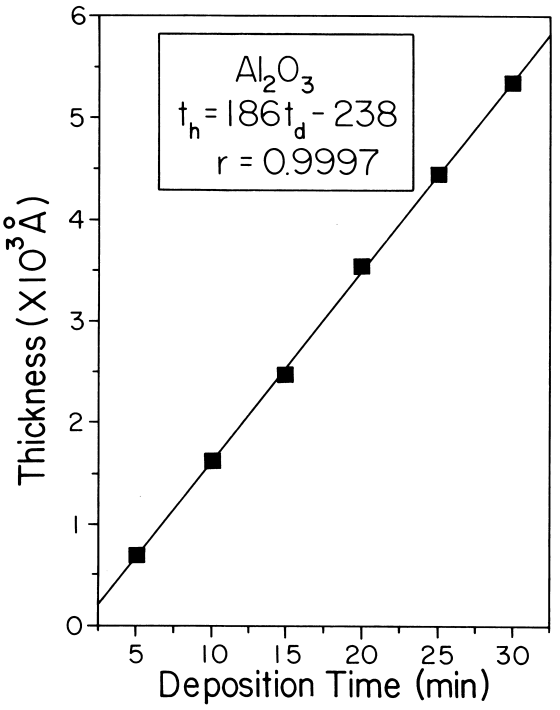

Fig. 1. Thickness as a function of deposition time for aluminum oxide films prepared by pyrosol at substrate temperature of 480°C.

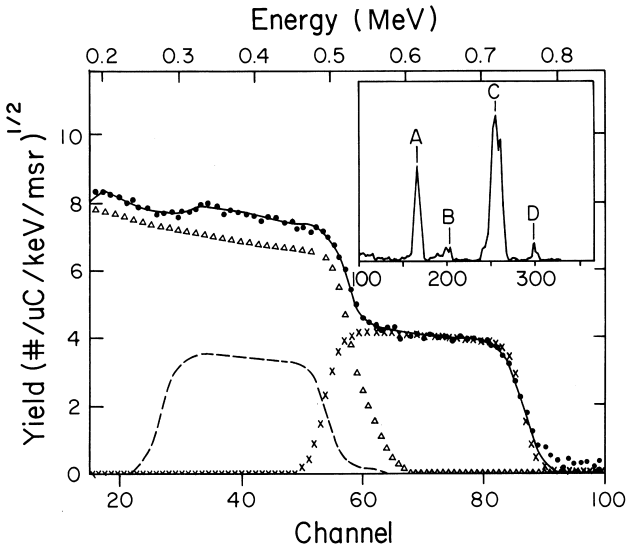

Fig. 2. A 1.7 MeV $^4He^+$ backscattered energy spectrum (dots) from an aluminum oxide films prepared at substrate temperature of 510°C. The continuos line is the RUMP simulated spectrum. The individual Al (×), O (−) and Si (△) scattering yield contribution to the simulated spectrum are also shown. The inset shows the NR particle yields of the following NR. A: $^{16}O(d_1p_1)^{17}O^*$; B: $^{16}O(d_1\alpha_0)^{14}N$; C: $^{16}O(d_1p_0)^{17}O$; D: $^{12}C(d_1p_0)^{13}C$.

thickness of the deposited films measured by ellipsometry and by profilometry; both thickness values are similar. These n values indicate that the deposited films are constituted by a material with a non-stoichiometric chemical composition, being aluminum deficient, or it can be due to the amorphicity of the films. In general, it is known that for several metal-rich oxides the refractive index is higher than that obtained for the stoichiometric material [15].

Fig. 2 shows a typically backscattered $^4He^+$ spectrum of 1.7 MeV ions incident at angle 0° with respect to the normal on the aluminum oxide film deposited on a c-Si substrate at $T_s = 510$°C. A similar spectrum was obtained for films deposited at 480°C. A quantitative analysis of the RBS spectra was made using the well-known 'RUMP' software [16]. The analysis consist of a simulation of each spectrum (solid line) and its comparison with the experimental one (dots). Fig. 2 also shows the individual Al, O and Si counting scattering yield contribution to the simulated spectrum. Table 2 shows some typical results of the films' atomic density in monolayer units (10^{15} atoms/cm^2) for the Al and O, and the Al/O ratio obtained from the RUMP simulation.

Table 1
Refractive index and thickness of aluminum oxide films[a]

T_s (°C)	t_{he} (nm)	n	t_{hp} (nm)
480	163.2	1.647	163.8
510	143.5	1.648	144.7

[a] t_{he} and t_{hp} are the values of the thickness obtained by ellipsometry and profilometry, respectively.

It can be observed from Fig. 2, that the oxygen scattering yield Y_O can be obtained from the total scattering yield Y_t by taking out the silicon yield Y_{Si} in the region of interest. If Y_O is used to calculate the oxygen concentration in the film, it has a large fractional statistical error ($\cong$ 20%) because Y_{Si} is considered as background yield and $Y_{Si} << Y_O$. However, the RUMP simulation does not use the Y_O yield to obtain the oxygen concentration in the aluminum oxide film. The oxygen concentration is obtained by the lack of Al scattering yield in the Al energy region due to the O in the film. The RUMP errors for the O and Al concentration determinations are about 6% [16] This procedure has been used in similar problems to obtain the chemical composition of binary compounds, when one of the elements is much heavier than the other, such as aluminum nitride and silicon carbide, on substrates heavier than the medium light element [12].

The inset in Fig. 2 shows NR peaks produced by 0.94 MeV $^2H^+$ and $\theta = 165°$ of the same sample. The following NR peaks from the oxygen were identified as: $^{16}O(d,p_1)O^{17}*$ (peak A), $^{16}O(d,\alpha)N^{14}$ (peak B), $^{16}O(d,p_0)O^{17}$ (peakC) and $^{12}C(d,p)C^{13}$ (peak D). The carbon peak is due to beam carbon built-up at the surface of the sample because the scattering chamber vacuum was relatively low ($\cong 5 \times 10^{-5}$ Torr) and it is not oil-free. The NR particle count yields can be used to obtain the oxygen per cm^2 on the films, if the NR cross-section of each peak is provided. The $^{16}O(d,p_1)O^{17}*$ cross-section was used here to calculate the oxygen content in the films, because it has a well-known

Table 2
Some typical results of the oxygen and aluminum atomic densities (10^{15} atoms/cm^2) and the O/Al ratio of the films, obtained from the RUMP simulation; the oxygen areal densities obtained from the NR $^{16}O(d_1p_1)^{17}O^*$ are shown for comparison with the RBS results

Sample temperature (°C)	Al (10^{15}, atoms/cm^2) RBS	O (10^{15}, atoms/cm^2) RBS	O/Al ratio RBS	O (10^{15}, atoms/cm^2) NR
480	1201 ± 72	2092 ± 125	1.74 ± 0.2	2210 ± 220
510	1238 ± 74	1912 ± 115	1.54 ± 0.2	2146 ± 215

value of 11.91 mb/sr and it is almost constant for $^2H^+$ energies between 0.938 and 0.980 MeV [17].

Table 2 also shows the results of the films' oxygen/cm^2 measured with the NR. It can be observed that the NR oxygen areal density measurements are in agreement with the RBS calculated values. The existence of this nuclear reaction indicates that there is no contamination of the deposited films with residual carbon from the aluminum material source, aluminum acetylacetonate. However, in all the analyzed samples, the deposited film is associated with an oxygen-rich material. The observed trend for the measured chemical composition and refractive index has been reported for films prepared by other techniques using different aluminum materials as source [18]. The peak *D* is related with carbon build-up due to the radiation because the vacuum system used in these measurements is not oil-free.

Fig. 3 shows the infrared transmission spectra for films deposited onto crystalline silicon at a substrate temperature of 480°C for deposition times of 15 min (Fig. 3a) and 60 min (Fig. 3b). In these spectra a broad band located from 400 to 1000 cm^{-1} is observed. This absorption band is characteristic of Al_2O_3 film and it is composed by the contribution of the vibrations of aluminum oxide which change their shape, position and transition probability depending on the chemical form of the aluminum oxidation [19]. A peak located at 1060 cm^{-1} is also observed. This peak, located at 1060 cm^{-1}, which is well defined for the thinner film (Fig. 3a), is associated with absorption due to the stretching vibration mode of the Si–O bond, which for stoichiometric silicon dioxide is located at 1070 cm^{-1}. The existence of SiO_2 is explained by the formation of a transition layer in the interface between the silicon substrate and the deposited aluminum oxide film. The observed shift toward low wavenumber is explained by the deviations from the stoichiometry of the silicon oxide in the interface which is a silicon-rich oxide [20]. This peak almost disappear for the thicker film. It is important to remark that signals due to absorption by O–H groups at 3900–3945 cm^{-1}, absorption related to alanol groups (Al–OH) at 3200–3470 cm^{-1} or absorption peaks located at 2000–1250 cm^{-1} associated with water, are not observed in the spectra obtained for the as-deposited films. It is known that the surface of the Al_2O_3 film becomes active at high substrate temperatures (≥450°C) and also that porous aluminum oxide films in which certain impurities are incorporated during growth show a high sensitivity to water adsorption on their surfaces [14]. However, IR transmittance measurements carried out in our same samples, after at least 2 months kept at air atmosphere and room temperature, show identical spectra to those shown in Fig. 3. These results indicate that the deposited material is chemically stable and that it is a dense material, although the chemical composition indicates an oxygen-rich material.

Fig. 4 shows the optical transmission curves in the range from 190 to 900 nm, for film prepared at $T_s = 480$°C onto fused quartz (Fig. 4a) and onto pyrex glass slices (Fig. 4b),

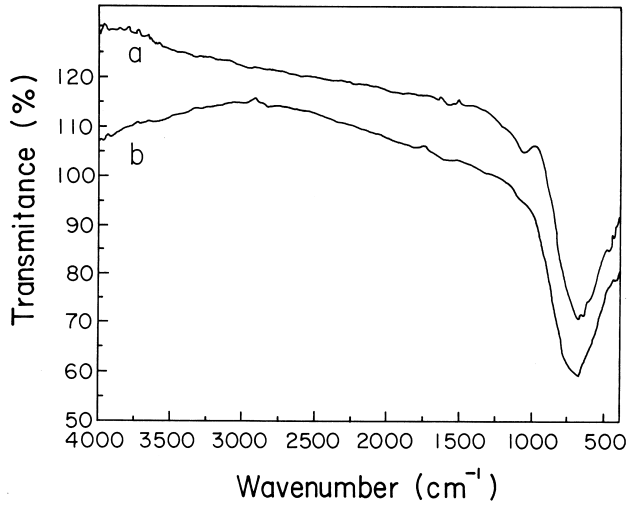

Fig. 3. Infrared spectra for films deposited at $T_s = 480$°C with deposition time of 15 min (a) and 60 min (b).

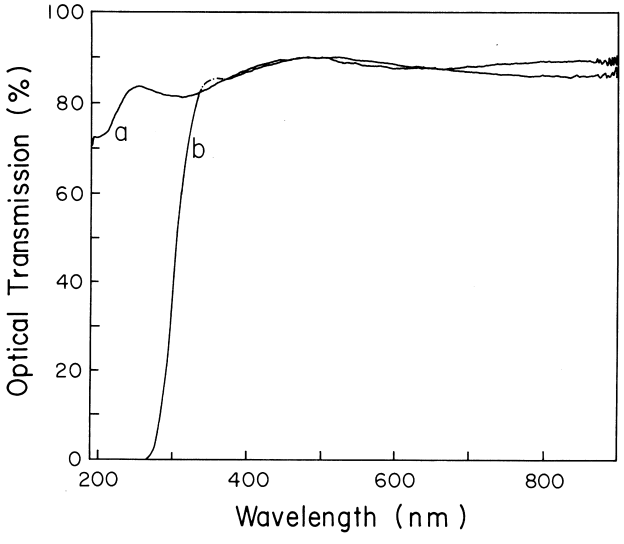

Fig. 4. Optical transmission for samples deposited at 480°C onto pyrex glass (a) and onto fused quartz (b).

both films with similar thickness (≅ 234 nm). The optical transmission measured is about 88% in the range from 400 to 900 nm and the deposited films appear transparent and colorless. Similar results have been reported for aluminum oxide films deposited by other techniques onto substrates of the same kind [14,18]. Although reflectance measurements were not made, the spectrum in Fig. 4a, for the film deposited onto fused quartz, does not show the absorption edge associated with transition through the energy band gap. This fact indicates that the energy band gap of the aluminum oxide deposited films is wider than 6.2 eV ($\lambda = 200$ nm). The high value measured for the optical transmission is associated with a high optical quality of the material, which is advantageous for applications in opto-electronic devices, and on the other hand, this value is similar to those reported earlier for films deposited by PECVD and thermal CVD at similar substrate temperatures.

Fig. 5 shows the electrical characteristics of a metal/insulator/metal structure with the aluminum oxide film deposited at substrate temperature of 480°C with a thickness of 202 nm onto glass coated with Sb-doped tin oxide conducting contact. This substrate is similar to that used to prepare electroluminescent devices as has been reported [21]. From Fig. 5 it can be observed that the current density measured for electric fields below 2 MV/cm is on the order of 10^{-10} A/cm^2 and it is associated with displacement current due to the applied voltage ramp. For electric fields higher than 2 MV/cm a ledge in the density current is observed. This behavior is related with current injection across the insulating layer.

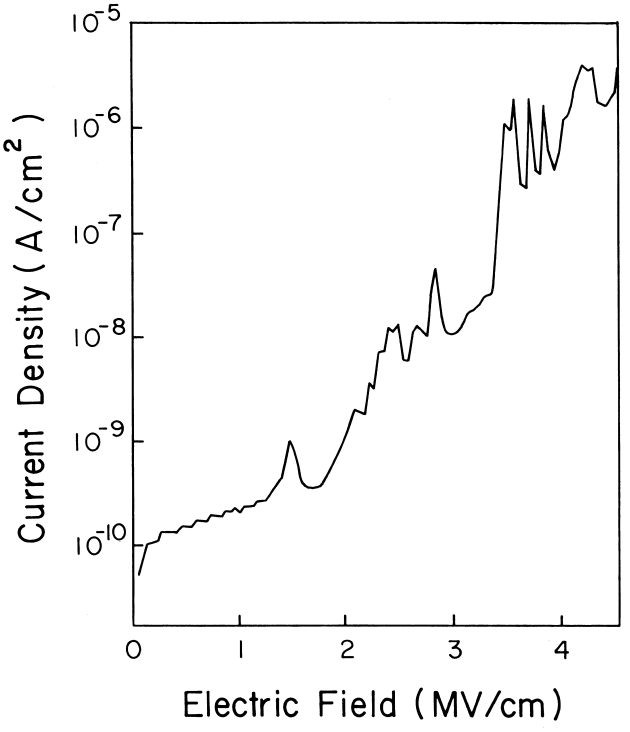

Fig. 5. Current density electric field characteristics of a MIM structure with an incorporated aluminum oxide film.

The electrical resistivity, in this voltage region, is about 10^{14} Ω cm; this value is higher by six or seven orders of magnitude than those values measured in porous aluminum oxide films. There are some peaks on this curve associated with local breakdown. The current density increases up to values on the order of 10^{-6} A/cm^2 at electric fields of about 4.5 MV/cm. It should be remarked that no destructive breakdown was observed at the high values of current density and electric fields reached.

4. Conclusions

Aluminum oxide films prepared by the pyrosol process at substrate temperatures of 480–510°C, using acetylacetonate as source material, show good microstructural and electric insulating properties. In general, the aluminum oxide films result in a non-stoichiometric relative chemical composition being formed by an oxygen-rich material as is indicated by the oxygen/aluminum ratio calculated from the RBS measurements, with values of the refractive index of 1.647 and 1.648, respectively. From infrared spectra, the existence of a broad band from 400 to 1000 cm^{-1} due to vibrations of Al_2O_3 is observed. There are no absorption peaks related with the incorporation of O–H or alanol (Al–OH) groups, even in IR measurements taken 2 months after keeping the samples in air atmosphere at room temperature. Films deposited onto pyrex glass and fused quartz slices show high optical transmission of about 88% in the wavelength range from 400 to 900 nm. These optical transmission measurements indicate that the energy band gap has a value higher than 6.2 eV. The electrical characteristics indicate that the films have electrical resistivity on the order of 10^{14} Ω cm and that a real current injection across the film is observed for applied electric fields higher than 2 MV/cm. Electric breakdown for electric fields up to 4.5 MV/cm was not observed. In summary, stable aluminum oxide films with microstructural, optical and electrical properties suitable to be applied in opto-electronic devices have been deposited by the pyrosol process.

Acknowledgements

The authors wish to thank M.A. Canseco, L. Huerta, E.P. Zavala and S. Jimenez for technical assistance. This work was partially supported by DGAPA-UNAM under Project IN100997. The CN accelerator Van de Graaff laboratory operation was partially supported by DGAPA-UNAM under project IN108798.

References

[1] E. Ciliberto, I. Fragala, R. Rizza, G. Spoto, G.C. Allen, Appl. Phys. Lett. 67 (1995) 1624.
[2] K.P. Pande, V.K.R. Nair, D. Gutierrez, J. Appl. Phys. 54 (1983) 5436.

[3] Y.A. Ono, in: G.L. Trigg (Ed.), Electroluminescence, Encyclopedia of Applied Physics, Vol. 5, Wiley-VCH, Berlin, 1993, p. 295.
[4] V.K. Khanna, R.K. Nahar, Appl. Surf. Sci. 28 (1987) 247.
[5] J.S. Kim, H.A. Marzouk, P.S. Reucroft, J.D. Robertson, C.E. Hamrin Jr., Appl. Phys. Lett. 62 (1993) 681.
[6] T. Maruyama, T. Nakai, Appl. Phys. Lett. 58 (1991) 2079.
[7] Z. Banamara, B. Gruzza, Mater. Chem. Phys. 39 (1994) 85.
[8] M. Tiitta, E. Nykanen, P. Soininen, L. Niinisto, M. Leskela, R. Lappalainen, MRS Bull. 33 (1998) 1315.
[9] A. Ortiz, J.C. Alonso, V. Pankov, D. Albarran, J. Luminesc. 81 (1999) 45.
[10] M. Langlet, J.C. Joubert, in: C.N.R. Rao (Ed.), Chemistry of Advanced Materials, Pyrosol Process or The Pyrolysis of an Ultrasonically Generated Aerosol, Blackwell Scientific, Oxford, 1993, p. 55.
[11] J.C. Viguie, J. Spitz. J. Electrochem. Soc. 122 (1975) 585.
[12] E. Andrade, J.C. Pineda, E.P. Zavala, F. Alba, S. Muhl, J.A. Zapien, J.M. Mendez, in: J.L. Duggan, I.L. Morgan (Eds.), Applications of Accelerators in Research and Industry, Denton, USA, November 6–9, 1996, American Institute of Physics Conference Proceedings, 392, AIP, New York, 1997, p. 616.
[13] T.W. Kim, S.S. Yom, W.N. Kang, et al., Appl. Surf. Sci. 65/66 (1993) 854.
[14] C.H. Lin, H.L. Wang, M.H. Hon, Surf. Coat. Technol. 90 (1997) 102.
[15] J.C. Alonso, A. Ortiz, C. Falcony, M. García, J. Vac. Sci. Technol. A 13 (1995) 244.
[16] L.R. Doolite, Nucl. Instrum. Methods Phys. Res. B 15 (1986) 227.
[17] G. Amsel, Nucl. Instrum. Methods 92 (1971) 484.
[18] T.S. Plaskett, P.P. Freitas, J.J. Sun, et al., in: J. Tobin, D. Chambliss, D. Kubinski, et al. (Eds.), Magnetic Ultrathin Films, Multilayers and Surfaces, San Francisco, CA, March 31– April 4, 1997, MRS Symp. Proc., 45, 1997, p. 469.
[19] T. Maruyama, S. Arai, Appl. Phys. Lett. 60 (1992) 322.
[20] P.G. Pai, S.S. Chao, Y. Takagi, G. Lucovsky, J. Vac. Sci. Technol. A 4 (1986) 689.
[21] A. Ortiz, J.C. Alonso, V. Pankov, J. Mater. Sci.: Mater. Electron. 10 (1999) 503.